A COMBINATION OF NEIGHBORHOOD BASED RATIO OPERATOR AND CONVOLUTIONAL WAVELET NEURAL NETWORKS FOR CHANGE DETECTION IN MULTI-TEMPORAL SYNTHETIC APERTURE RADAR IMAGES

Nguyen Hung An*, Nguyen Tien Phat
Le Quy Don Technical University

ARTICLE INFO

Received: 11/5/2021
Revised: 28/5/2021
Published: 31/5/2021

KEYWORDS

SAR image
Multi-temporal images
Difference image
Change detection
Ratio operator

ABSTRACT

Change detection in multi-temporal Synthetic Aperture Radar (SAR) images is widely utilized for practical applications of resource investigation, supervision, and management on sea and land with a large area. There is a variety of algorithms for the change detection using two multi-temporal SAR images. The popular principle of them is to analyze a difference image generated from these two images by a ratio operator to detect change areas between them. In order to improve detection accuracy, the ratio operator and modified versions of this operator are usually used in a combination with further fine processing solutions. This paper developed a novel solution of the change detection based on a combination of the Neighbor-based Ratio operator and the Convolutional Wavelet Neural Network algorithm for improving the accuracy of change detection in multi-temporal SAR images.

PHÁT HIỆN SỰ THAY ĐỔI TRONG ẢNH SAR ĐA THỜI GIAN BẰNG CÁCH KẾT HỢP TOÁN TỬ TỶ SỐ DỰA TRÊN LÂN CẬN VÀ MẠNG NƠ RON TÍCH CHẬP WAVELET

Nguyễn Hùng An*, Nguyễn Tiến Phát
Trường Đại học Kỹ thuật Lê Quý Đôn

THÔNG TIN BÀI BÁO

Ngày nhận bài: 11/5/2021
Ngày hoàn thiện: 28/5/2021
Ngày đăng: 31/5/2021

TỪ KHÓA

Ảnh SAR
Ảnh đa thời gian
Ảnh sai khác
Phát hiện sự thay đổi
Toán tử tỷ số

TÓM TẮT

Phát hiện sự thay đổi trong ảnh SAR đa thời gian được ứng dụng rộng rãi trong các ứng dụng thực tế về hoạt động quản lý kiểm tra, giám sát tài nguyên trên đất liền và trên biển với quy mô rộng lớn. Có rất nhiều thuật toán phát hiện sự thay đổi sử dụng hai ảnh SAR đa thời gian. Nguyên tắc phổ biến của chúng là thực hiện phân tích ảnh sai khác được tạo ra từ toán tử tỷ số của hai ảnh SAR đa thời gian nhằm phát hiện các sự thay đổi giữa chúng. Để cải thiện độ chính xác phát hiện, toán tử tỷ số và các phiên bản cải tiến của toán tử này thường được sử dụng kết hợp với các phương pháp xử lý tinh hơn nữa. Bài báo này đề xuất một giải pháp phát hiện sự thay đổi bằng cách kết hợp toán tỷ số dựa trên lân cận và thuật toán mạng nơ ron wavelet tích chập để cải thiện độ chính xác phát hiện sự thay đổi trong ảnh SAR đa thời gian.

DOI: https://doi.org/10.34238/tnu-jst.4476

* Corresponding author. *Email: hungan@lqdtu.edu.vn*

1. Introduction

Research on change detection in multi-temporal SAR images has been received great interests for recent decades. For being hardly impacted by weather conditions, the SAR images are very popular used in resource surveillance and management systems in wide areas on sea and land. Algorithms of multi-temporal SAR image change detection are basically implemented through the three following stages: image pre-processing, difference image (DI) generation, and DI analysis. A great challenge in processing SAR images is to limit effects of speckle noise inherently existed in them on detection accuracy. While the first stage corrects geometry of two SAR images and matches them together, the remaining two stages focus on filtering the speckle noise and identify the changed areas based on the DI image.

To reduce impacts of the speckle noises, which are multiplicative ones, on the detection performance, the DIs are mainly generated by ratio or log-ratio operators from the two multi-temporal images instead of traditional subtraction operator. According to the logarithm property, these operations transform the multiplicative speckle noises into the additive ones. Therefore, it is easier to remove these noises by filters. In 2011, Gong et al. [1] proposed a neighbor-based-ratio (NR) operator to create DI images for change detection in SAR images. This operator exploits gray level and spatial information of neighbor pixels in the DI generation, and so produces the better DIs in terms of speckle noise suppression than those created by traditional subtraction, ratio, and log-ratio operators.

In spite of using the log-ratio operator or its modified versions, speckle noise effects in the DI image are not still completely removed. Therefore, in the third stage, DI analysis, continues to reduce these effects for more accurate change detections. DI analysis algorithms are various, but can be divided into four basic types: threshold-based, clustering based, transform based, neural network based methods. In addition, in recent years, there has been a research trend on combining these types together to improve detection accuracy.

For the threshold based methods, an optimal threshold of image intensity is chosen from the DI's histogram to classify image pixels into changed and unchanged classes [2]-[4]. The clustering based methods group similar pixels into one region (or cluster) based on some certain criteria. K-means clustering algorithm is a typical example of these methods [5], [6]. However, Fuzzy-C-means (FCM) clustering algorithm, which is a soft k-means one, is the most widely used clustering one [7]-[9]. In this algorithm, each data point can belong to more than one cluster with different weights. In comparison with the threshold based methods, the clustering based methods are more flexible, but have the same disadvantage of noise sensitivity. Although, both threshold and clustering based methods are simple in calculation and implementation, but their accuracy is all very limited.

Transform based methods are usually applied after DI generation stage. They take special features of transforms such as Discrete Wavelet transform [10], [11], Randon transform [12], Fourier transform [13] etc. to select distinctive and salient regions from the DIs. However, algorithms of change detection in SAR images using transforms are frequently combined with other solutions to increase their accuracy. In 2018, Gao et al. [14] proposed a method of change detection in SAR images using Frequency Domain Analysis and Random Multi-Graphs (FDA-RMG). In this algorithm, the Fourier transform was used to coarsely localize changed regions, while the random multi-graphs in combination with the FCM algorithm were implemented for a further refined identification of changed regions from the potential candidates.

In recent years, using artificial neural network in change detection in SAR images has received great considerations [15], [16] and is considered as a finally processing step to improve accuracy of the detection. In 2016, Gao et al. [17] proposed a method of change detection in SAR images based on the combination of neighbour-based-ratio operator and extreme learning machine NR-ELM). In 2019, an approach based on Convolutional-Wavelet Neural Networks

(CWNN) [18] was also developed by these authors, in which the convolutional neural network (CNN) [19] is combined with the dual tree complex wavelet transform (DT-CWT) [20] for change detection.

This paper developed a novel algorithm of change detections in SAR images, which is a combination of the NR operator and CWNN method. For instance, in the proposed method, the NR operator is used to create the DI image, while CWNN is performed to finely classify change regions from potential candidates. The remainder of the paper is organized as follows. Section 2 presents the methodology for the proposed method. In Section 3, we present some simulation results to evaluate the proposed algorithm performance in comparison with three other algorithms. In Section 4, we draw conclusions from the results of our evaluation and outline research areas for future work.

2. Research methodology

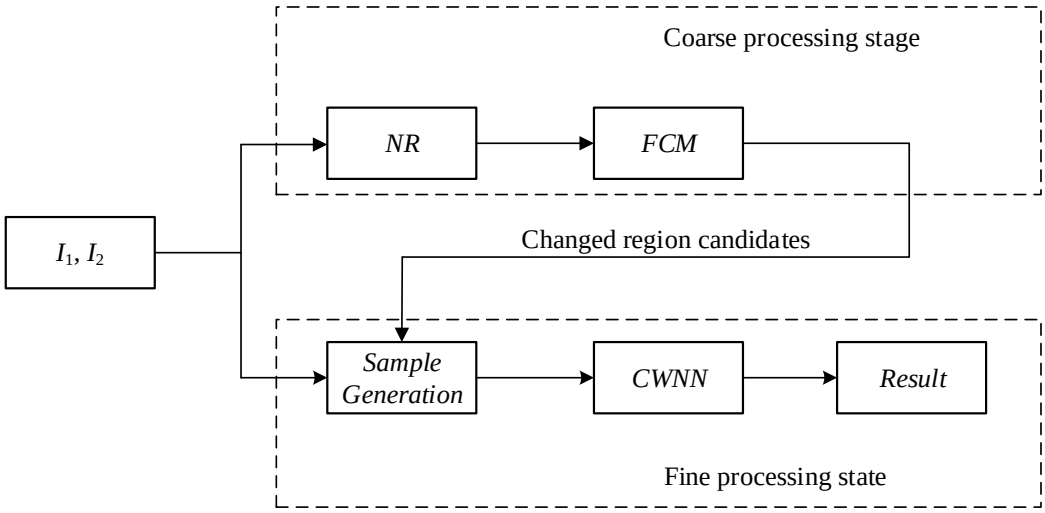

Figure 1. *The block diagram of the proposed method*

Exploiting the spatial relation of neighbor pixels in two SAR images makes the NR operator advantageous over the traditional ratio ones in generating the DIs in terms of speckle noise suppression. Furthermore, the CWNN algorithm is proved as a power tool to suppress speckle noises in the DI and identify changed regions. Therefore, combining them could be an effective approach for accuracy improvement of change detection in multi-temporal SAR images. Because the proposed algorithm was developed as a combination of the NR operator and CWNN technique, thus it is named as the NR-CWNN method for convenience. This section describes the implementation of the proposed method in detail. The block diagram of this method is shown in Figure 1.

In this diagram, I_1 and I_2 are two multi-temporal SAR images, in which I_2 is a changed version of I_2. It was assumed that the geometric correction and registration for these two images were obtained. The NR-CWNN algorithm was implemented through two stages as follows. In the first stage, called the coarse processing stage, the DI image was created by using neighbour-ratio (NR) operator [1]. For instance, the NR operator is defined as follows:

$$DI(x) = \frac{\sigma(x)}{\mu(x)} \times \frac{\min\left(I_1(x), I_2(x)\right)}{\max\left(I_1(x), I_2(x)\right)} + \left(1 - \frac{\sigma(x)}{\mu(x)}\right) \times \frac{\sum_{i \in \Omega \cap i \neq x} \min\left(I_1(x), I_2(x)\right)}{\sum_{i \in \Omega \cap i \neq x} \max\left(I_1(x), I_2(x)\right)} \quad (1)$$

where $DI(x)$ denotes the gray level of a pixel on the position x on the DI image created from two multi-temporal SAR images $I_1(x)$ and $I_2(x)$. $\sigma(x)$ and $\mu(x)$ are respectively gray level variance

and mean in neighbourhood Ω_x. From the DI image, candidates of changed region were selected by Fuzzy-C-Means (FCM) algorithm [7], [8] for further processing.

In the second stage, called the fine processing stage, the CWNN [18] was utilized to identify changed regions. The inputs of CWNN are image patches including training sample and virtual sample patches created by the block *Sample generation*. In order to avoid effects of the limited number of training samples, virtual samples were generated in this block, and were behaved as training ones. In fact, CWNN is a combination of the dual tree complex wavelet transform (DT-CWT) with the convolutional neural network (CNN). The DT-CWT helps to keep low frequency sub-bands and suppress high-frequency sub-bands of the images. As a result, some speckle noises of high frequency are suppressed. In addition, CNN was utilized to train image patches for further change classification.

3. Simulation results and discussion

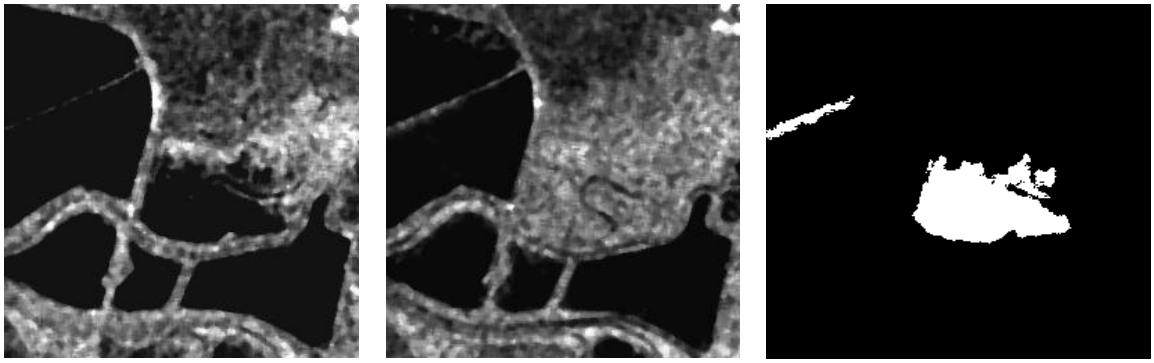

(a) (b) (c)

Figure 2 . *San Francisco images (a) acquired in August 2003, (b) acquired in May 2004, and (c) map of changed areas (ground truth) used as a reference in simulations. The ground-truth image was created by integrating prior information with photo interpretation*

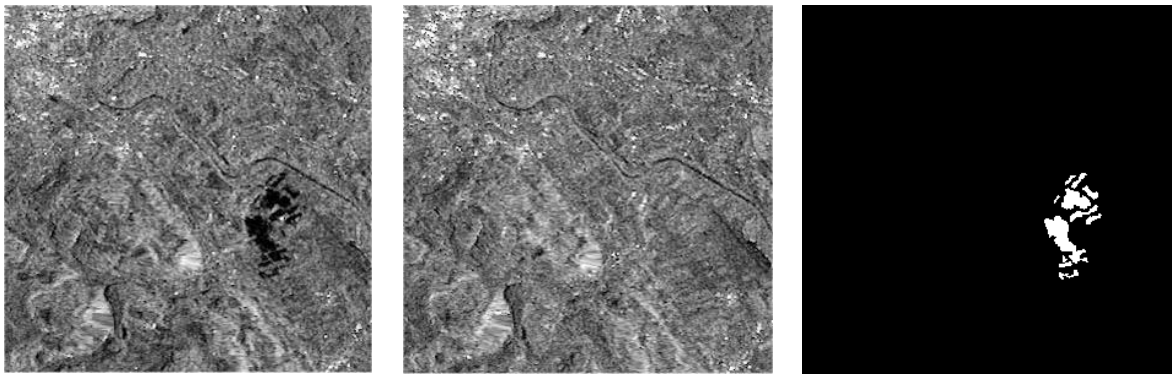

(a) (b) (c)

Figure 3 . *The multi-temporal SAR images of Bern city (a) acquired in April 1999, (b) acquired in May 1999, and (c) ground truth image. The ground-truth image was created by integrating prior information with photo interpretation*

The simulation was implemented on two datasets shown in Figure 2 and Figure 3. The first dataset is two original multi-temporal SAR images of San Francisco acquired by the ERS-2 SAR sensor in 2003 and 2004 (see Figure 2(a) and (b)). These images have the size of 7749x7713 pixels. For simple computation, their two corresponding sections with the size of 256x256 pixels were investigated. The second dataset is the images of the Bern city captured before and after a flood in 1999 (see Figure 3(a) and (b)). The section of the images used for the simulation has the size of 301x301 pixels.

The performance evaluation of the proposed method was implemented in qualitative and quantitative ways based on Matlab simulation for these two datasets. For instance, the simulation result images of the proposed, FDA-RMG, CWNN and NR-ELM methods were compared with the corresponding ground-truth maps, which were obtained by integrating prior information with photo interpretation (Figure 2(c) and Figure 3(c)). The simulation result images are difference ones (or binary images) with 1 referring to changed pixels and 0 referring to unchanged pixels. In other words, the white presents changed pixels, and the black describes unchanged pixels.

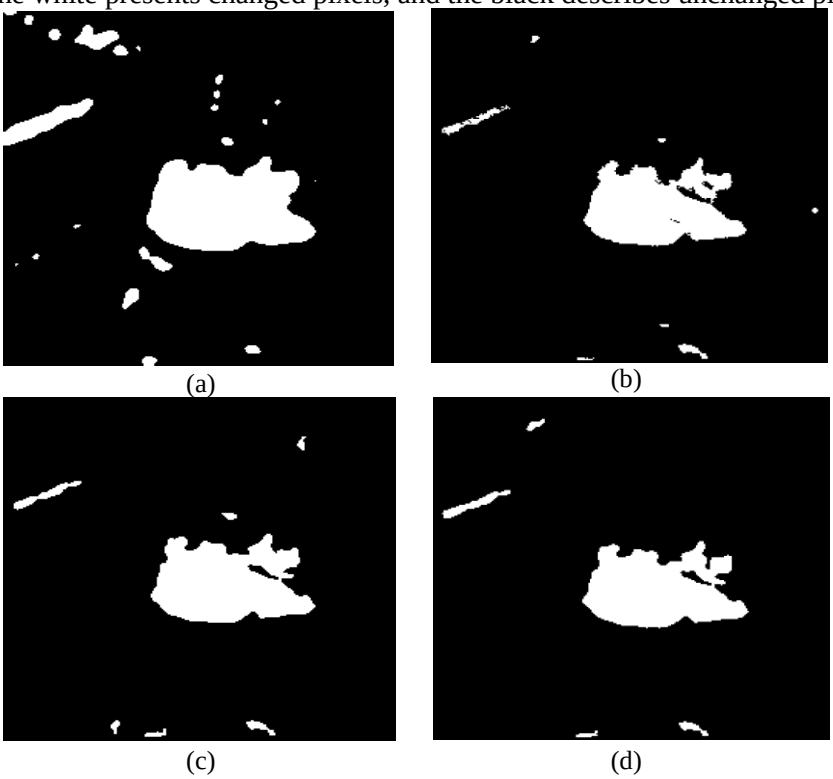

Figure 4. *Qualitative analysis results of performance of (a) FDA-RMG method, (b) NR-ELM method, (c) CWNN method, and (d) proposed method. The results are achieved for the images of San Franciso in Figure 2*

For the qualitative performance evaluation, the binary images created by FDA-RMG, CWNN, NR-ELM and proposed methods were compared with the corresponding ground-truth images by human eyes. Particularly, the comparisons were performed by counting the number of white regions in the result images of each investigated method that do not exist in the ground truth image. In addition, the number of white regions in the ground truth image that do not exist in the result images of each compared method was counted. The sum of these two numbers is the total number of wrongly detected white regions by the investigated method. The simulation results were shown in Figure 4 and Figure 5. Figure 4 shows the change maps achieved by the four algorithms for the two SAR images in Figures 2(a) and (b). As seen from Figure 4 in comparison with the ground truth image in Figure 2(c), the change detection result of the proposed method is better than the three remaining methods. For instance, the change maps detected by the proposed method has three wrongly detected regions, while the number of wrongly detected regions of FDRMG, NR-ELM, and CWNN methods are respectively 18, 6, 5. Similarly, the simulation results in Figure 5 for the second dataset of Bern city in Figure 3 show that the proposed method gives the qualitatively better result than FDA-RMG and NR-ELM methods. For instance, it is obvious that Figure 5(a) created by FDA-RMG method is the most different among four result images compared to the ground truth image. Figure 5(b) created by NR-ELM method has a white

region that does not exist in the ground truth image. Figure 5(c) and Figure 5(d) respectively produced by CWNN and proposed methods look similar to the ground truth image.

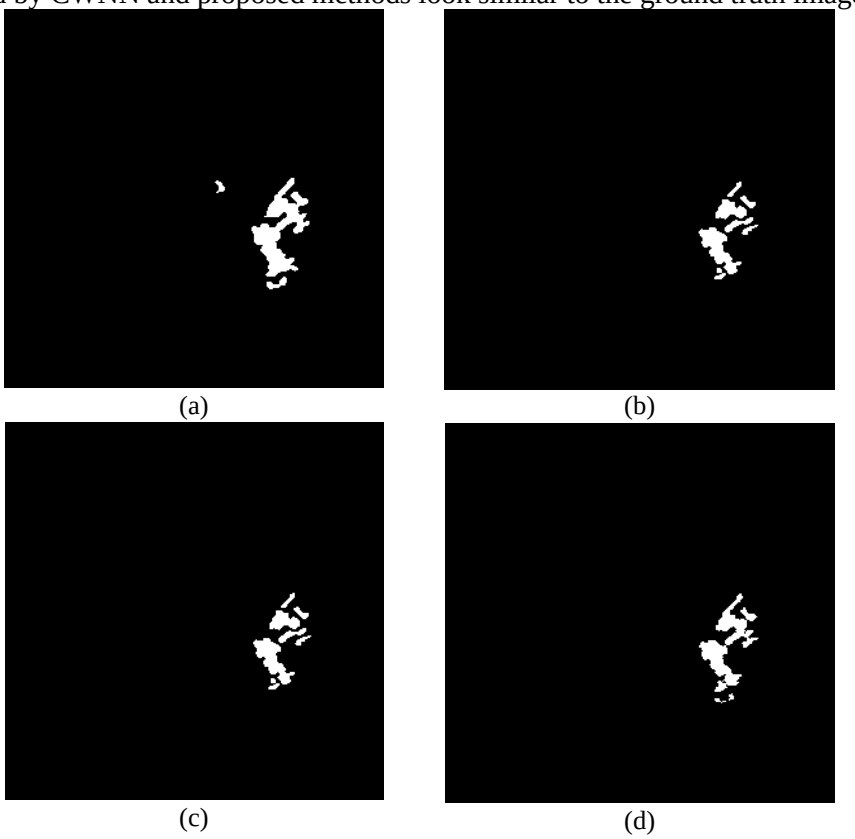

Figure 5. *Qualitative analysis results of performance of (a) FDA-RMG method, (b) NR-ELM method, (c) CWNN method, and (d) proposed method. The results are achieved for the images of Bern city in Figure 3*

In addition, quantitative analyses were performed for these four methods by four criteria: false positives (FP), false negatives (FN), overall error (OE), and percentage correct classification (PCC). For instance, the four parameters are defined as follows. FP is the number of unchanged pixels (black pixels) in the ground truth image but wrongly classified as changed ones (white pixels), while FN is the number of changed pixels in the ground truth image wrongly classified as unchanged ones in the result images. OE is summation of FP and FN:

$$OE = FP + FN \tag{2}$$

PCC is computed in percentage as follows.

$$PCC = \frac{N - OE}{N} \times 100(\%) \tag{3}$$

where N is the total pixels in the ground truth image.

The quantitative performance evaluations of these four methods were presented in the Table 1 and Table 2. Here, Table 1 lists the four parameters computed by using first dataset of San Francisco in Figure 2, while Table 2 present the four parameters calculated by using the second dataset of Bern City in Figure 3. It can be seen from Table 1 that the proposed method achieved the best PCC result compared with the three other methods. For instance, the parameter PCC of proposed method is respectively improved 1.54 %, 0.14 %, and 0.08 % in comparison with FDA-RMG, NR-ELM, and CWNN methods. Similarly, Table 2 also shows that parameter of PCC achieved by the proposed method is the highest among the four investigated ones.

Table 1. *The quantitative comparison of performance of the proposed method with those of the three other methods using the images of San Francisco in Figure 2*

Methods	FP	FN	OE	PCC (%)
FDA-RMG	1610	30	1640	97.46
NR-ELM	217	550	767	98.82
CWNN	437	295	732	98.88
Proposed	447	234	681	98.96

Table 2. *The quantitative comparison of performance of the proposed method with those of the three other methods using the images of Bern city in Figure 3*

Methods	FP	FN	OE	PCC (%)
FDA-RMG	247	119	366	90.60
NR-ELM	146	194	340	99.62
CWNN	235	75	310	99.65
Proposed	170	100	270	99.69

Through Matlab simulation and achieved results, it can be concluded that the proposed method provides the highest accuracy of change detection in comparison with the FDA-RMG, NR-ELM, and CWNN methods.

4. Conclusion

The paper developed a novel method for detecting changes in multi-temporal SAR images based on neighbor-ratio analysis and the CWNN method. The proposed method was performed through two stages from the coarse to the fine level. In the coarse processing stage, the neighbour-ratio operator was firstly applied for the two images to create the DI image, then, the FCM algorithm was computed on the DI image to identify the changed region candidates. In the fine processing stage, the CWNN method was used to train image samples generated from these candidates for refined change detection results.

The results of performance evaluation based on the Matlab simulation showed that the proposed method improves accuracy in comparison with recent developed methods. However, its complexity was the highest among the compared algorithms. In the near future, our research orientation will focus on simplifying computational procedures to increase processing speed of the proposed change detection algorithm.

REFERENCES

[1] M. Gong, Y. Cao, and Q. Wu "A neighborhood-based ratio approach for change detection in SAR images," *IEEE Geoscience and Remote Sensing Letters*, vol. 9, pp. 307-311, 2011.

[2] J. Kittler and J. Illingworth, "Minimum error thresholding," *Pattern recognition*, vol. 19, pp. 41-47, 1986.

[3] G. Moser and S. B. Serpico, "Generalized minimum-error thresholding for unsupervised change detection from SAR amplitude imagery," *IEEE Transactions on Geoscience and Remote sensing*, vol. 44, pp. 2972-2982, 2006.

[4] M. N. Sumaiya and R. S. Selva Kumari, "Logarithmic mean-based thresholding for SAR image change detection," *IEEE Geoscience and Remote Sensing Letters*, vol. 13, pp. 1726-1728, 2016.

[5] J. MacQueen, "Some methods for classification and analysis of multivariate observations," *Proceedings of the fifth Berkeley symposium on mathematical statistics and probability*, 1967, pp. 281-297.

[6] T. Celik, "Unsupervised change detection in satellite images using principal component analysis and *k*-means clustering," *IEEE Geoscience and Remote Sensing Letters*, vol. 6, pp. 772-776, 2009.

[7] J. C. Dunn, "A fuzzy relative of the ISODATA process and its use in detecting compact well-separated clusters," *Journal of Cybernetics*, vol. 3, pp. 32-57, 1973.

[8] J. C. Bezdek "Objective function clustering," *Pattern recognition with fuzzy objective function algorithms*, Springer, pp. 43-93, 1981.

[9] M. Gong, Z. Zhou, and J. Ma, "Change detection in synthetic aperture radar images based on image fusion and fuzzy clustering," *IEEE Transactions on Image Processing*, vol. 21, pp. 2141-2151, 2011.

[10] H. Zhuang, K. Deng, Y. Yu, and H Fan, "An approach based on discrete wavelet transform to unsupervised change detection in multispectral images," *International Journal of Remote Sensing*, vol. 38, pp. 4914-4930, 2017.

[11] T. Celik and K. K. Ma, "Multitemporal image change detection using undecimated discrete wavelet transform and active contours," *IEEE Transactions on Geoscience and Remote Sensing*, vol. 49, pp. 706-716, 2010.

[12] J. Zheng and H. You, "A new model-independent method for change detection in multitemporal SAR images based on Radon transform and Jeffrey divergence," *IEEE Geoscience and Remote Sensing Letters*, vol. 10, pp. 91-95, 2012.

[13] Y. Q. Cheng, H. C. Li, T. Celik, and F. Zhang, "FRFT-based improved algorithm of unsupervised change detection in SAR images via PCA and K-means clustering," *Proceedings of 2013 IEEE International Geoscience and Remote Sensing Symposium-IGARSS*, pp. 1952-1955, 2013.

[14] F. Gao, X. Wang, J. Dong, and S. Wang, "Synthetic aperture radar image change detection based on frequency-domain analysis and random multigraphs," *Journal of Applied Remote Sensing*, vol. 12, pp. 1-17, 2018.

[15] Y. Duan, F. Liu, L. Jiao, P. Zhao, and L. Zhang, "SAR Image segmentation based on convolutional-wavelet neural network and markov random field," *Pattern Recognition*, vol.64, pp. 255-267, 2017.

[16] G. B. Huang, H. Zhou, X. Ding, and R. Zhang, "Extreme learning machine for regression and multiclass classification," *IEEE Transactions on Systems, Man, and Cybernetics, Part B (Cybernetics)*, vol.42, pp. 513-529, 2011.

[17] F. Gao, J. Dong, B. Li, Q. Xu, and C. Xie, "Change detection from synthetic aperture radar images based on neighborhood-based ratio and extreme learning machine," *Journal of Applied Remote Sensing*, vol.10, pp. 1-14, 2016.

[18] F. Gao, X. Wang, Y. Gao, J. Dong, and S. Wang, "Sea ice change detection in SAR images based on convolutional-wavelet neural networks," *IEEE Geoscience and Remote Sensing Letters*, vol.16, pp. 1240-1244, 2019.

[19] K. O'Shea and R. Nash, "An introduction to convolutional neural networks," *arXiv preprint arXiv:1511.08458*, pp. 1-11, 2015.

[20] I. W. Selesnick, R. G. Baraniuk, and N. C. Kingsbury, "The dual-tree complex wavelet transform," *IEEE signal processing magazine*, vol.22, pp. 123-151, 2005.